

Release notes for NASA-produced MERIS and OLCI cyanobacteria index (CI_{cyano}) data product to support the Cyanobacteria Assessment Network (CyAN) Project



Table of Contents

Version History	1
Overview of data files and processing	2
Processing version and reprocessing schedule	4
Version 6 improvements/changes	4
Known issues	13
References	15
Appendix A: CyAN Merged OLCI metadata V6	17
Appendix B: CyAN MERIS metadata V5	20
Appendix C: CyAN MERIS metadata V4	23

Version History

This is version 6; Feb 2025

Four U.S. federal agencies – EPA, NASA, NOAA, and USGS – collaborated to form the Cyanobacteria Assessment Network (CyAN) Project. This work is supported by the NASA Ocean Biology and Biogeochemistry Program/Applied Sciences Program (proposal 14-SMDUNSOL14-0001 and SMDSS20-0006) and by in-kind contributions from the U.S. EPA, NOAA, and the U.S. Geological Survey Toxic Substances Hydrology Program [Schaeffer *et al.*, 2015]. NASA's principal role in CyAN is the production, validation, and distribution of satellite-derived cyanobacteria index (CI_{cyano}) data products from the ESA Medium Resolution Imaging Spectrometer onboard Envisat (MERIS; 2002–2012) and Ocean Colour Land Imager onboard Sentinel-3A (OLCI; 2017–present) and Sentinel-3B (2018–present) for the continental United States (CONUS) and Alaska (Table 1). This document accompanies NASA's production of CI_{cyano} data products for MERIS and OLCI.

Table 1. Agency roles and responsibilities.

Agency	Role
EPA	Satellite application methods for management of freshwater HABs and water quality
NASA	Satellite data processing, evaluation/validation, quality control
NOAA	Satellite algorithms to detect and forecast HABs for marine systems and Great Lakes
USGS	Field freshwater HAB monitoring, ecological expertise, Landsat satellite management

Overview of data files and processing

As detailed metadata for each file can be found in Appendix A, this section provides only top-level details on file format and content. Briefly, the NASA Ocean Biology Processing Group (OBPG; <https://oceancolor.gsfc.nasa.gov>) at Goddard Space Flight Center (GSFC) generated the MERIS and OLCI CI_{cyano} data files. The CI_{cyano} algorithm is fully described in [Wynne et al. \[2008\]](#), [Wynne et al. \[2010\]](#), and [Coffer et al. \[2020\]](#), [Seegers et al. \[2022\]](#). Daily and 7-day composites of CI_{cyano} are available at 300-m resolution. These images were transformed to Albers Equal Area projection with an area-weighted interpolation to match the projections of the National Hydrography Dataset. Shuttle Radar Topography Mission (SRTM) 60-meter data provided the land mask (https://dds.cr.usgs.gov/srtm/version2_1/SWBD/). The CI_{cyano} value in each pixel represents the maximum CI_{cyano} value for both the daily and 7-day composite periods. CONUS and Alaska composites are divided into and delivered as a regional numbered tile (Figure 1 and Figure 2), representing a spatial area made into a separate file. The data file name will use the column and row number to identify the tile location.

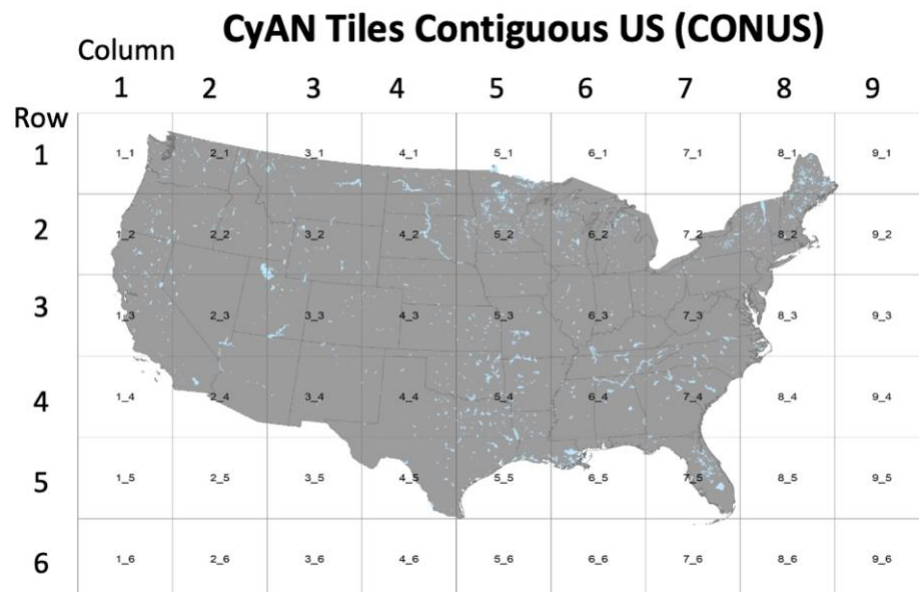


Figure 1. Envisat and Sentinel-3 CONUS satellite tiles (9X6 tiles)

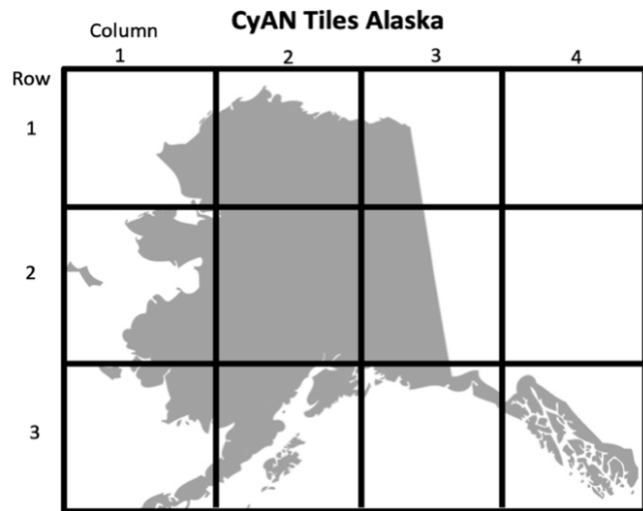


Figure 2. Envisat and Sentinel-3 Alaska satellite tiles (4x3 tiles). A lower resolution land mask is used for the Alaska region (landmask_GMT15ARC_AK_v2021.nc)

Each data file is stored in 8-bit GeoTIFF, where values of:

- 0 indicate below threshold CI_{cyan} detection limits
- 1-253 are data
- 254 is land
- 255 are no data (e.g., a cloudy pixel, ice cover)

Digital numbers (DN) can be converted to an estimated cyanobacteria abundance derived from CI_{cyan} . $CI_{cyan} = 10^{**}(DN * 0.011714 - 4.1870866)$

MERIS/OLCI data files follow this naming convention:

sensoryyyydddyyyyddd.datalevel_temporalresolution_product_version_resolution_region

A file named *M20120642012070.L3m_7D_CYAN_CI_cyan_CYAN_CONUS_300m_5_3*, for example, is decomposed as:

- sensor: *M* = MERIS, *L* = OLCI
- *yyydddyyddd* : *20120642012070* = year 2012 day 064 to year 2012 calendar day 070
- datalevel: *L3m* = satellite processing level-3, mapped image
- temporalresolution: *7D* = 7-day temporal composite, DAY = daily maximum
- product: Project identifier *CI_cyan* (*CI cyanobacteria product*), *tc* (*true color*)
 - CONUS products: CYAN_CI_cyan, CyANTC_tc
 - Alaska products: CYANAK_CI_cyan, CYANAKTC_tc
- version: *CYAN_CONUS*, *CYAN_AK* (Alaska)

- resolution : $300m$ = pixel resolution
 - region : 5_3 = tile column (5) and row (3)
- * The Alaska naming conventions follows a similar pattern with the single difference of “AK” replacing “CONUS” in the file name.

In addition to the 7-day composites and dailies for CI_{cyano}, daily true color images are also provided. The OLCI products are merged Sentinel-3A and 3B from 2018-present. Data for MERIS are provided as 14-day composites from 2002-2007, when the instrument irregularly viewed the US and as 7-day composites and dailies from 2008-2012, when the instrument regularly collected data over the US. Daily true color images are also provided for CONUS and Alaska for MERIS and OLCI with 2018 true colors being a composite of OLCI Sentinel-3A and 3B.

These data are validated Stage 2 of 4 on NASA’s data maturity level ranking. This is defined as “data product accuracy is estimated using a significant set (although not full US/global) of independent measurements obtained from selected locations and time periods and ground-truth/field program efforts. There have been some peer-reviewed publications on the accuracy, but for limited spatial areas.” Additional details on NASA’s data maturity levels can be found at <https://science.nasa.gov/earth-science/earth-science-data/data-maturity-levels>.

For details on data product validation efforts and applications, see *Binding et al. [2011]*, *Matthews et al. [2012]*, *Moradi [2014]*, *Lunetta et al. [2015]*, *Matthews and Odermatt [2015]*, *Palmer et al. [2015a]*, *Palmer et al. [2015b]*, *Tomlinson et al. [2016]*, *Urquhart et al. [2017, 2019]*, *Clark et al. [2017]*, *Schaeffer et al. [2018]*, *Mishra et al. [2019]*, *Coffer et al. [2020]*, *Stroming et al. [2020]*, *Seegers et al. [2022]*, *Whitman et al. [2022]*.

Processing version and reprocessing schedule

All data are processing version 6 (February 2025). Data are preliminary and to be used for evaluation purposes only. Known outstanding issues are listed below.

The CyAN Project and OBPG will periodically reprocess and redistribute the MERIS and OLCI CI_{cyano} time-series. Reprocessing will occur every 10 to 16 months.

Version 6 improvements/changes

The following improvements have been implemented in version 6 (February 2025).

1. Updated processing to use the latest NASA S3A and S3B vicarious calibration with minor adjustments to the 681 nm and 709 nm wavelengths
2. Implemented water vapor correction as part of atmospheric correction
3. Improved test for turbid waters, which reduces false positive CI_{cyano} detection in turbid environments

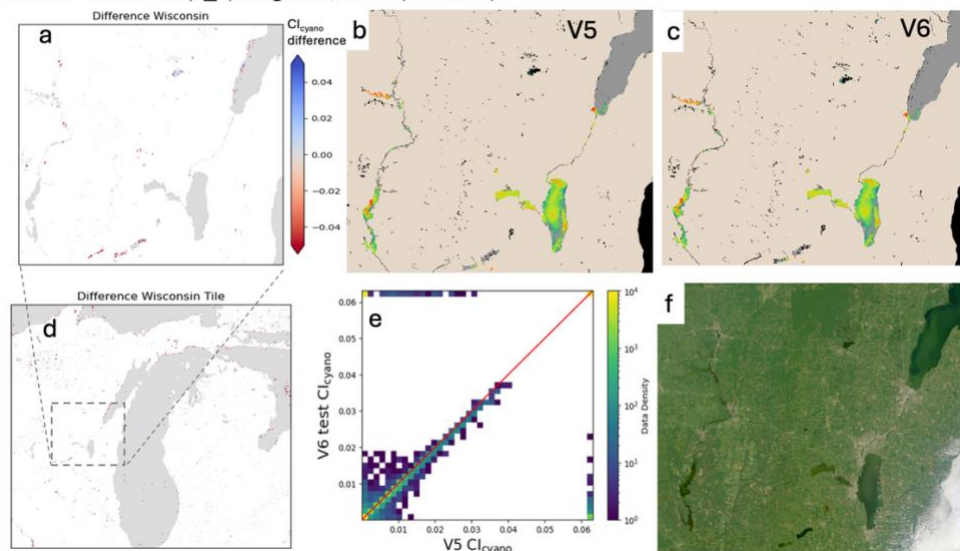
Summary of Analysis

- The changes have minor impact at the low-end and tends to slightly reduces CI_{cyano} values at the high-end.
- The turbid water change should reduce false positives in turbid waters.

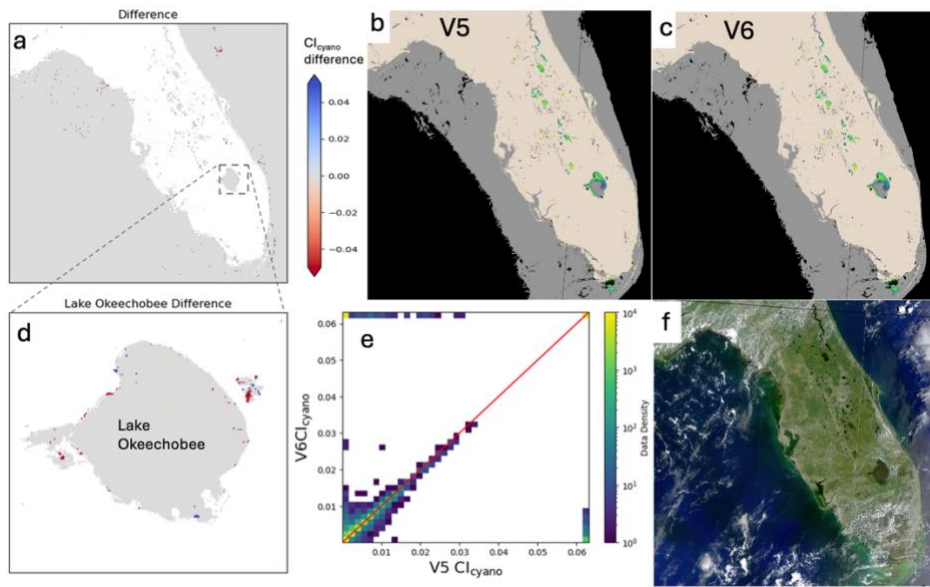
Examples of V5 vs. V6

The following imagery and analysis help highlight the impact of code and processing changes from CyAN V5 to V6 on different regions around CONUS. The imagery may show the entire tile or a selected region or body of water. The scatter plots comparing V5 to V6 CI_{cyano} values are data for the entire tile.

Central Wisconsin (6_2) August 5, 2022 (2022217)

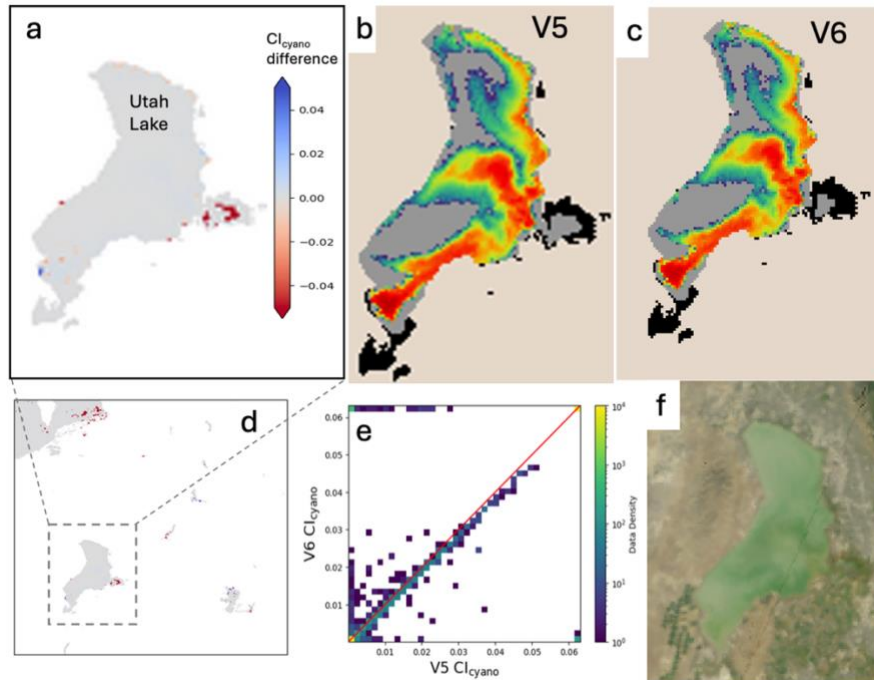


Florida tile (7_5) August 20, 2022 (2022232)



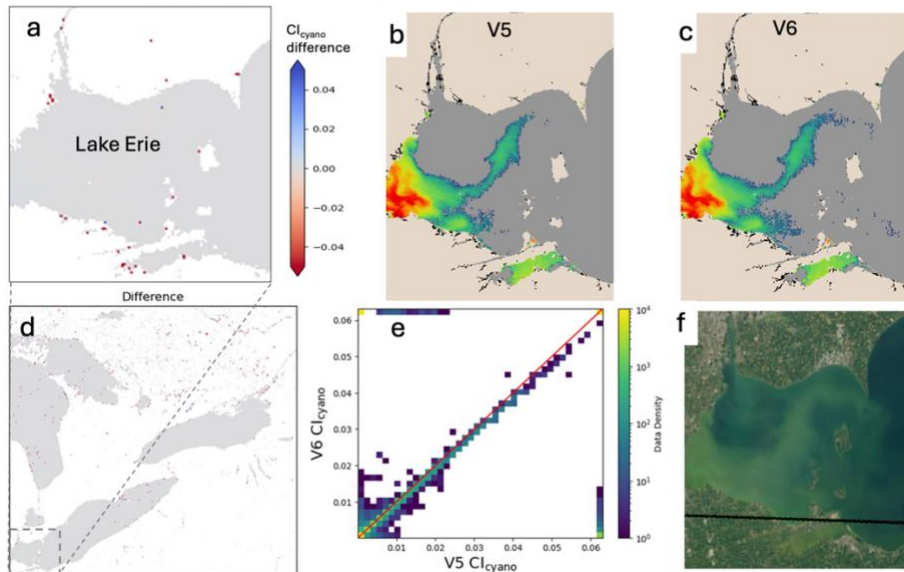
Difference maps from 20 August 2022 for the Florida Tile (6_2; a) and a focus on the Lake Okeechobee area (d) highlighting changes at the pixel level between version 5 and version 6. Red indicates a V6 increase in Cl_{cyano} . Corresponding Cl_{cyano} imagery maps for version 5 (b) and version 6 (c) are shown. A scatterplot summarizing differences between V5 and V6 Cl_{cyano} values for the Florida tile with color indicating data density (e). True color (f).

Utah Lake (3_3) August 24, 2022 (2022236)



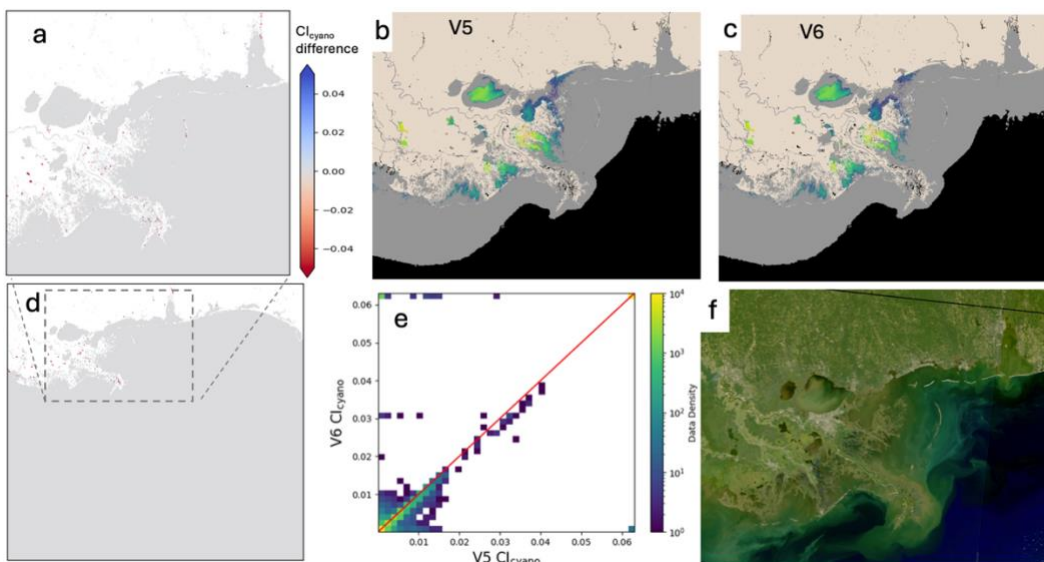
Difference maps from 24 August 2022 highlighting changes at the pixel level between version 5 and version 6 for Utah Lake (a) and the full Utah region tile (d). Red indicates increase in V6. Corresponding Cl_{cyano} imagery version 5 map (b) and version 6 map (c) are shown. A scatterplot summarizing differences between V5 and V6 Cl_{cyano} values for the Utah Lake tile (3_3) the color indicates data density (e). True color (f).

Lake Erie Tile (7_2) August 24, 2022 (2022236)



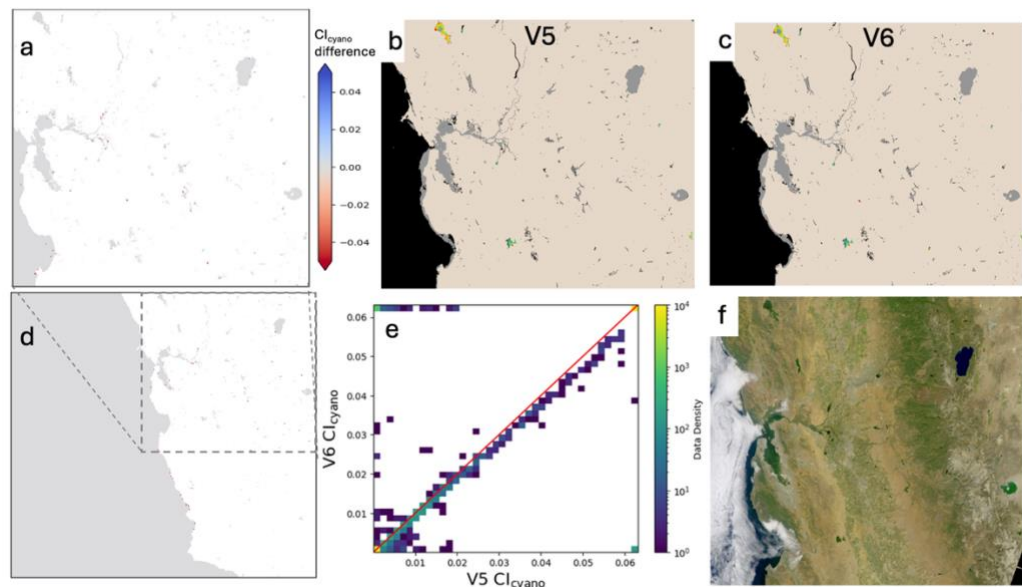
Difference maps from 24 August 2022 highlighting changes at the pixel level between version 5 and version 6 for Lake Erie (a) and the regional tile (d). Red indicates increase in V6. Corresponding mapped CI_{cyano} imagery for Lake Erie version 5 (b) and version 6 (c) are shown. The scatterplot summarizes differences between V5 and V5 CI_{cyano} values for the regional tile (7_2) with color indicating data density (e). True color (f).

Lake Pontchartrain Tile (6_5) October 1, 2022 (2022274)



Difference maps for 1 October 2022 highlighting changes at the pixel level between version 5 and version 6 for Lake Pontchartrain (a) and the regional tile (d). Red indicates increase in V6. Corresponding mapped CI_{cyano} imagery for Lake Pontchartrain and the surrounding area version 5 (b) and version 6 (c). The scatterplot summarizes differences between V5 and V6 CI_{cyano} values for the full regional tile (7_2) with color indicating data density (e). True color (f).

Central California Tile (1_3) August 27, 2022 (2022239)



Difference maps for 27 August 2022 for a region including San Francisco Bay (a) and the central California tile (d) highlighting pixel level changes between version 5 and version 6. Red indicates a V6 increase in Cl_{cyano} . Corresponding Cl_{cyano} imagery maps for version 5 (b) and version 6 (c). A scatterplot summarizing differences between V5 and V6 Cl_{cyano} values for the central California tile with color indicating data density (e). True color (f).

Previous Versions

Version 5 improvements/changes

The following improvements have been implemented in version 5 (May 2023).

1. This version includes an improved filter for turbid water exclusion, which reduces CI_{cyano} values in highly turbid environments.
2. Correction to clear water correction when retrieved K_d is invalid.
3. Applied OLCI to MERIS inter-calibration for CI (Wynne et al., 2021)
4. Updated gains now using ESA's Collection-3 vicarious calibration.

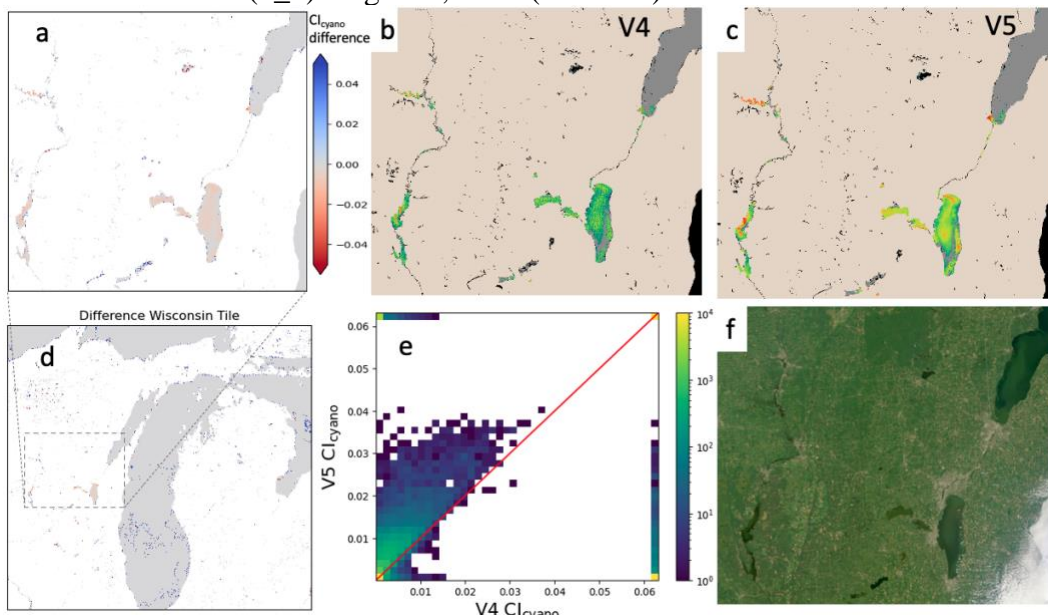
Summary of Analysis

- The calibration changes should increase sensitivity at low-end and have limited impact at high-end.
- A change in the binning process in how maximum values are selected has led to general increase in CI_{cyano} values, especially in the 7-day composite products.
- Version 5 shows on average a 15-20% increase in CI_{cyano} values. This is driven by gain changes (using updated ESA gains)
- The turbid water change should reduce false positives in turbid waters.

Examples of V5 vs. V4

The following imagery and analysis help highlight the impact of code and processing changes from CyAN V4 to V5 on different regions around CONUS. The imagery may show the entire tile or a selected region or body of water. The scatter plots comparing V4 to V5 CI_{cyano} values are data for the entire tile.

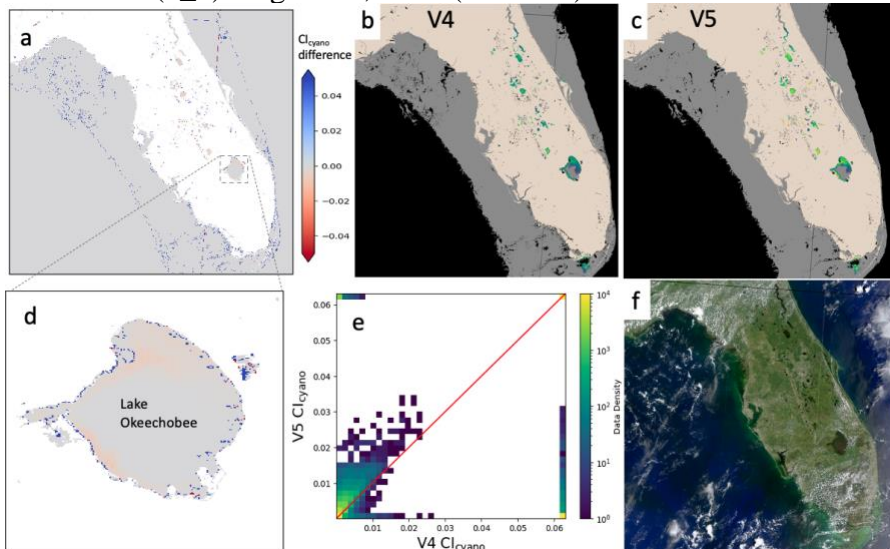
Central Wisconsin (6_2) August 5, 2022 (2022217)



Difference maps from 5 August 2022 for the Lake Winnebago area (a) and Wisconsin Tile (b)

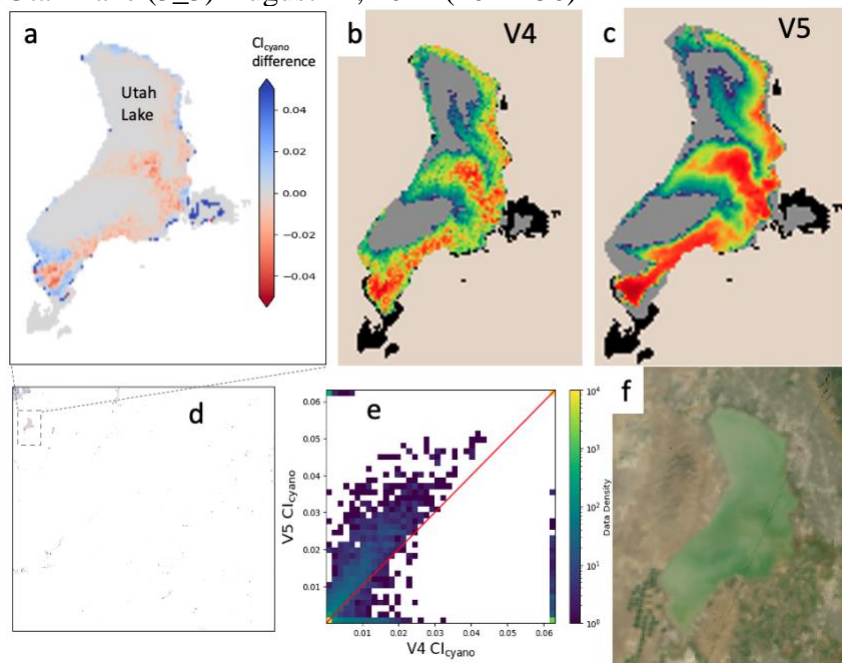
highlighting changes at the pixel level between version 4 and version 5. Red indicates a V5 increase in CI_{cyano} . Corresponding CI_{cyano} imagery maps for version 4 (b) and version 5 (c) are shown. A scatterplot summarizing differences between V4 and V5 CI_{cyano} values for the Wisconsin tile with color indicating data density (e). True color (f).

Florida tile (7_5) August 20, 2022 (2022232)



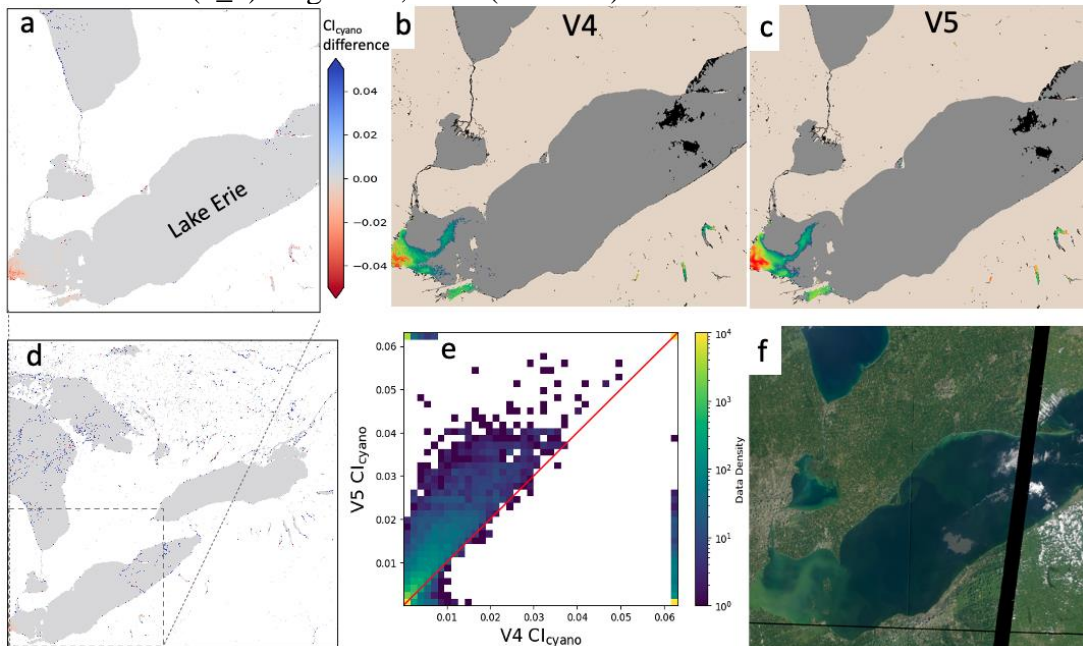
Difference maps from 20 August 2022 for the Florida Tile (6_2; a) and a focus on the Lake Okeechobee area (d) highlighting changes at the pixel level between version 4 and version 5. Red indicates a V5 increase in CI_{cyano} . Corresponding CI_{cyano} imagery maps for version 4 (b) and version 5 (c) are shown. A scatterplot summarizing differences between V4 and V5 CI_{cyano} values for the Florida tile with color indicating data density (e). True color (f).

Utah Lake (3_3) August 24, 2022 (2022236)



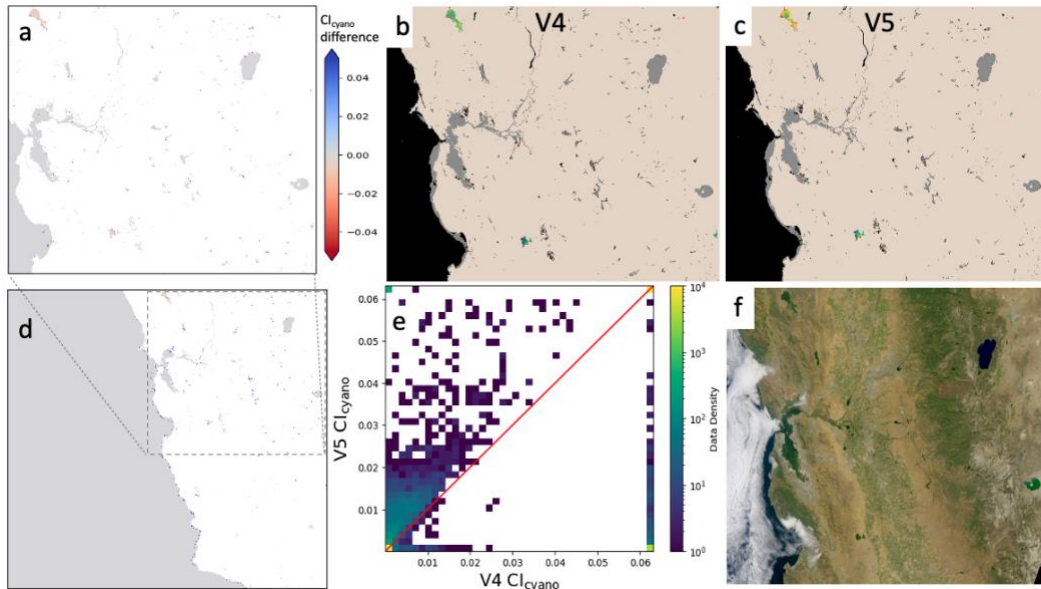
Difference maps from 24 August 2022 highlighting changes at the pixel level between version 4 and version 5 for Utah Lake (a) and the full Utah region tile (d). Red indicates increase in V5. Corresponding CI_{cyano} imagery version 4 map (b) and version 5 map (c) are shown. A scatterplot summarizing differences between V4 and V5 CI_{cyano} values for the Utah Lake tile (3_3) the color indicates data density (e). True color (f).

Lake Erie Tile (7_2) August 24, 2022 (2022236)



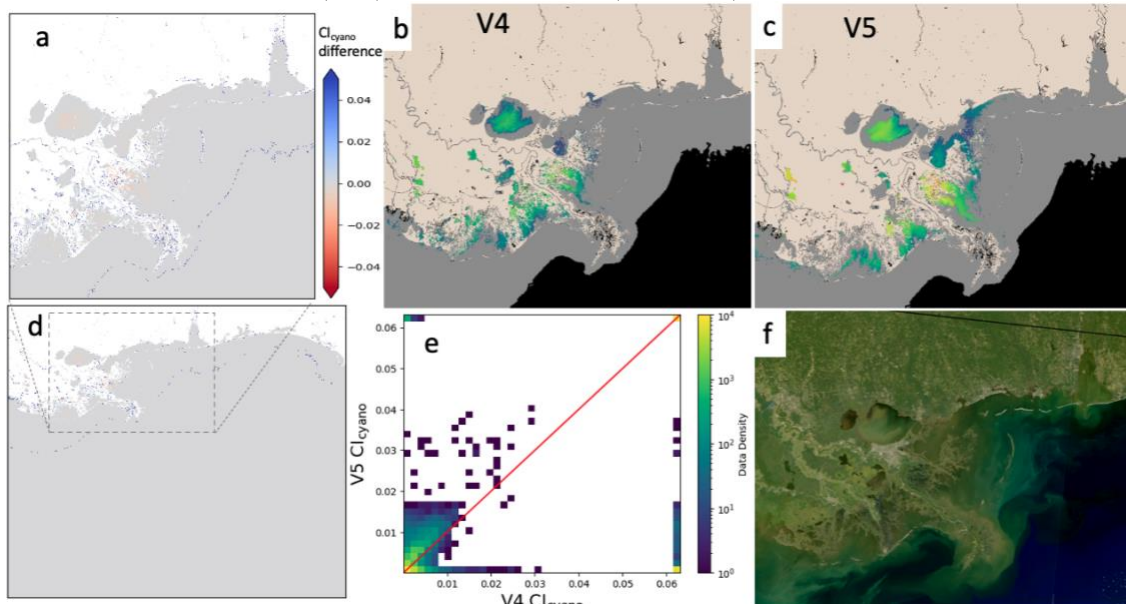
Difference maps from 24 August 2022 highlighting changes at the pixel level between version 4 and version 5 for Lake Erie (a) and the regional tile (d). Red indicates increase in V5. Corresponding mapped CI_{cyano} imagery for Lake Erie version 4 (b) and version 5 (c) are shown. The scatterplot summarizes differences between V4 and V5 CI_{cyano} values for the regional tile (7_2) with color indicating data density (e). True color (f).

Central California Tile (1_3) August 27, 2022 (2022239)



Difference maps for 24 August 2022 for a region including San Francisco Bay (a) and the central California tile (d) highlighting pixel level changes between version 4 and version 5. Red indicates a V5 increase in Cl_{cyano} . Corresponding Cl_{cyano} imagery maps for version 4 (b) and version 5 (c). A scatterplot summarizing differences between V4 and V5 Cl_{cyano} values for the central California tile with color indicating data density (e). True color (f).

Lake Pontchartrain Tile (6_5) October 1, 2022 (2022274)



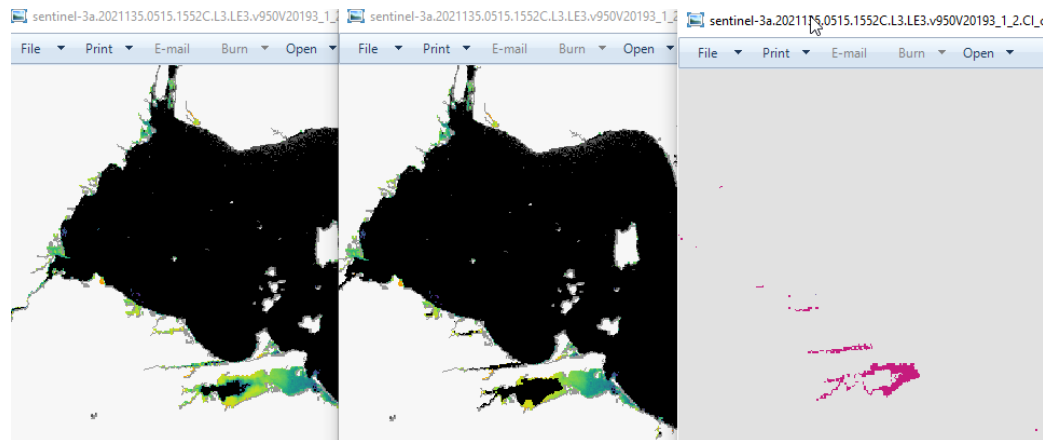
Difference maps for 1 October 2022 highlighting changes at the pixel level between version 4 and version 5 for Lake Pontchartrain (a) and the regional tile (d). Red indicates increase in V5. Corresponding mapped Cl_{cyano} imagery for Lake Pontchartrain and the surrounding area version 4 (b) and version 5 (c). The scatterplot summarizes differences between V4 and V5 Cl_{cyano} values for the full regional tile (7_2) with color indicating data density (e). True color (f).

Version 4 improvements/changes

The following improvements have been implemented in version 4 (March 2022).

1. Improvements include detection of false positive CI's in highly turbid waters
2. Flagging high glint.

V4 - An example from S3A on 3/15/2021 that highlights the difference between V3 and V4 with the turbidity correction with old CI turbidity (left), the turbidity improvement (middle), and the difference in red between detect and nondetect (right).



Version 3 improvements/changes

The following improvements have been implemented in version 3.

1. This version includes a merged OLCI CI_{cyano} product combining the data from Sentinel-3A and Sentinel-3B from 2018-present. The merged product is the maximum value for each pixel. The utilization of two satellites greatly increases spatial and temporal coverage relative to the previous sentinel-3A coverage only.
2. True color daily imagery from 2018-present use a combined imagery from S3A and S3B OLCI. If there is sensor swath overlap the true color image shows the mean value.
3. The land mask has been updated with an improvement in Ohio and South Dakota lakes.
4. The GEOTiffs now include product version information in metadata
5. There was a switch made to area weighted binning. Area weighting uses the intersection of the pixel geometry and the bin geometry (in lat/lon space) as a weighting factor when adding the pixel value into the bin. Each pixel is added to all bins that it intersects. The old binning scheme added the pixel to the closest bin using the center lat/lon location of each. Each pixel is only added to one bin. The area weighting makes a much nicer picture. For example, if the pixel area is bigger than the bin area, then you will end up with lots of empty bins using the old method.
6. Code fixes have been made to improve masking, especially nearshore potentially stray light contaminated pixels.

7. The 39 degree zenith angle filter was removed for OLCI, which increased the number of pixel recovered. The filter was put in place for MERIS, but is not necessary for OLCI.
8. In the imagery non-detect values (e.g. below detection threshold) have been color-separated from no data values (e.g., a cloudy pixel). Non-detects are grey and no data are black.
9. Lake Pontchartrain coastal masking error removed resulting in full lake CI coverage.
10. More nearshore CONUS coast will be processed.

Known Issues

The following issues will be addressed or resolved in future releases of these data.

- (1) A snow/flag that identifies ice has been applied, but has not yet been verified. Ice can potentially register as high CI counts, so caution should be used where snow/ice might be visible. It is currently unknown if CyAN could detect cyanobacteria under thin ice in lakes and reservoirs.
- (2) The SRTM land mask may cover dry lakes, and may exclude other lakes. There is a need for an eroded landmask.
- (3) A flag has been added to identify mixed pixels that are potentially inclusive of land and water. The flag has not yet been verified, so caution should be used where mixed pixels may occur at the land/water interface.
- (4) Undetected thin clouds can potentially register as high CI counts (elevating CI beyond the minimum detect threshold value).
- (5) Retrievals are considered more robust for lakes ≥ 900 m window width as defined in *Clark et al. [2017]*. This 900 m window width provides a minimum of a 3 x 3-pixel array in a water body. Smaller water bodies and rivers are not masked and their data may be erroneous.
- (7) Satellite data processing does not account for changes in water levels due to cycles such as drought and flood.
- (8) Published US validation locations are Lake Erie, Florida, Ohio, Vermont, New Hampshire, Rhode Island, Connecticut, Massachusetts, Oregon, California, Indiana, New Jersey, New York, Utah, New Hampshire, Vermont, Maine, California, Oregon, and Idaho.

Difference CyAN and NOAA-produced products

We thought it may be worth including the following text regarding CyAN (NASA produced) and NOAA produced product differences with the release:

Known differences between NOAA/NCCOS and CyAN CI products

- Flagging
 - o NOAA/NCCOS land=252, invalid=251,253,254,255
 - o CyAN land=254, invalid=255
- Range of valid data values
 - o NOAA/NCCOS 0-250
 - o CyAN 0-253

Differences in pixel values will also be noted due to differences in binning/mapping methods and differences in land masks used.

References

- Binding, C. E., T. A. Greenberg, J. H. Jerome, R. P. Bukata, and G. Letourneau (2011), An assessment of MERIS algal products during an intense bloom in Lake of the Woods, *Journal of Plankton Research*, 33(5), 793-806, doi:10.1093/plankt/fbq133.
- Clark, J. M., B. A. Schaeffer, J. A. Darling, E. A. Urquhart, J. M. Johnston, A. R. Ignatius, M. H. Myer, K. A. Loftin, P. J. Werdell, and R. P. Stumpf (2017), Satellite monitoring of cyanobacterial harmful algal bloom frequency in recreational waters and drinking water sources, *Ecological Indicators*, 80, 84-95, doi:10.1016/j.ecolind.2017.04.046.
- Coffer, M.M, B.A. Schaeffer, J.A. Darling, E.A. Urquhart, W.B. Salls. (2020), Quantifying national and regional cyanobacterial occurrence in US lakes using satellite remote sensing *Ecological Indicators*, 111, 105976, doi:10.1016/j.ecolind.2019.105976
- Lunetta, R. S., B. A. Schaeffer, R. P. Stumpf, D. Keith, S. A. Jacobs, and M. S. Murphy (2015), Evaluation of cyanobacteria cell count detection derived from MERIS imagery across the eastern USA, *Remote Sensing of Environment*, 157, 24-34, doi:10.1016/j.rse.2014.06.008.
- Matthews, M. W., S. Bernard, and L. Robertson (2012), An algorithm for detecting trophic status (chlorophyll-a), cyanobacterial-dominance, surface scums and floating vegetation in inland and coastal waters, *Remote Sensing of Environment*, 124, 637-652, doi:10.1016/j.rse.2012.05.032.
- Matthews, M. W., and D. Odermatt (2015), Improved algorithm for routine monitoring of cyanobacteria and eutrophication in inland and near-coastal waters, *Remote Sensing of Environment*, 156, 374-382, doi:10.1016/j.rse.2014.10.010.
- Mishra, S., R.P. Stumpf, B.A. Schaeffer, P.J. Werdell, K.A. Loftin and A. Meredith. (2019), Measurement of Cyanobacterial Bloom Magnitude using Satellite Remote Sensing. *Scientific Report* 9, 18310 <https://doi.org/10.1038/s41598-019-54453-y>
- Moradi, M. (2014), Comparison of the efficacy of MODIS and MERIS data for detecting cyanobacterial blooms in the southern Caspian Sea, *Marine Pollution Bulletin*, 87(1-2), 311-322, doi:10.1016/j.marpolbul.2014.06.053.
- Palmer, S. C. J., et al. (2015a), Validation of Envisat MERIS algorithms for chlorophyll retrieval in a large, turbid and optically-complex shallow lake, *Remote Sensing of Environment*, 157, 158-169, doi:10.1016/j.rse.2014.07.024.
- Palmer, S. C. J., D. Odermatt, P. D. Hunter, C. Brockmann, M. Presing, H. Balzter, and V. R. Toth (2015b), Satellite remote sensing of phytoplankton phenology in Lake Balaton using 10 years of MERIS observations, *Remote Sensing of Environment*, 158, 441-452, doi:10.1016/j.rse.2014.11.021.
- Schaeffer, B. A., K. Loftin, R. P. Stumpf, and P. J. Werdell (2015), Agencies collaborate, develop a cyanobacteria assessment network, *EOS Trans. AGU*, 96(23), 16-20.

Schaeffer, B. A., S.W. Bailey, R.N. Conmy, M. Galvin, A.R. Ignatius, J.M. Johnston, E.A. Urquhart (2018), Mobile device application for monitoring cyanobacteria harmful algal blooms using Sentinel-3 satellite Ocean and Land Colour Instruments. *Environ. Model. Softw.*, 109: 93-103

Seegers, B. N., Werdell, P. J., Vandermeulen, R. A., Salls, W., Stumpf, R. P., Schaeffer, B. A., Owens, T. J., Bailey, S. W., Scott, J. P., & Loftin, K. A. (2021). Satellites for long-term monitoring of inland U.S. lakes: The MERIS time series and application for chlorophyll-a. *Remote Sens Environ*, 266, 1-14. <https://doi.org/10.1016/j.rse.2021.112685>

Stroming, S., Robertson, M., Mabee, B., Kuwayama, Y., & Schaeffer, B. (2020), Quantifying the Human Health Benefits of Using Satellite Information to Detect Cyanobacterial Harmful Algal Blooms and Manage Recreational Advisories in U.S. Lakes. *GeoHealth*, 4, e2020GH000254. doi: 10.1029/2020GH000254

Tomlinson, M. C., R. P. Stumpf, T. T. Wynne, D. Dupuy, R. Burks, J. Hendrickson, and R. S. Fulton (2016), Relating chlorophyll from cyanobacteria-dominated inland waters to a MERIS bloom index, *Remote Sensing Letters*, 7(2), 141-149, doi:10.1080/2150704x.2015.1117155.

Urquhart, E. A., B. A. Schaeffer, R. P. Stumpf, K. A. Loftin, and P. J. Werdell (2017), A method for examining temporal changes in cyanobacterial harmful algal bloom spatial extent using satellite remote sensing, *Harmful Algae*, 67, 144-152, doi:10.1016/j.hal.2017.06.001.

Urquhart, E.A., Schaeffer, B.A., (2019), Envisat MERIS and Sentinel-3 OLCI satellite lake biophysical water quality flag dataset for the contiguous United States. *Data in Brief*, 104826. doi.:10.1016/j.dib.2019.104826.

Wynne, T. T., R. P. Stumpf, M. C. Tomlinson, and J. Dyble (2010), Characterizing a cyanobacterial bloom in western Lake Erie using satellite imagery and meteorological data, *Limnology and Oceanography*, 55(5), 2025-2036, doi:10.4319/lo.2010.55.5.2025.

Wynne, T. T., R. P. Stumpf, M. C. Tomlinson, R. A. Warner, P. A. Tester, J. Dyble, and G. L. Fahnenstiel (2008), Relating spectral shape to cyanobacterial blooms in the Laurentian Great Lakes, *International Journal of Remote Sensing*, 29(12), 3665-3672, doi:10.1080/01431160802007640.

Wynne, Timothy & Mishra, Sachi & Meredith, Andrew & Litaker, Richard & Stumpf, Richard. (2021). Intercalibration of MERIS, MODIS, and OLCI Satellite Imagers for Construction of Past, Present, and Future Cyanobacterial Biomass Time Series. *Remote Sensing*. 13. 2305. 10.3390/rs13122305.

Appendix A: CyAN daily merged OLCI metadata V6

```
// global attributes:  
:product_name = "L2022206.L3b_DAY_CYANV6T.nc" ;  
:temporal_range = "7-hour" ;  
:start_orbit_number = 22127 ;  
:end_orbit_number = 33524 ;  
:date_created = "2025032023755000" ;  
:processing_version = "6T" ;  
:time_coverage_start = "2022-07-25T13:35:09.000Z" ;  
:time_coverage_end = "2022-07-25T20:10:06.000Z" ;  
:northernmost_latitude = 62.87891f ;  
:southernmost_latitude = 8.350261f ;  
:easternmost_longitude = -45.16392f ;  
:westernmost_longitude = -154.366f ;  
:geospatial_lat_max = 62.87890625 ;  
:geospatial_lat_min = 8.35026073455811 ;  
:geospatial_lon_max = -45.1639213562012 ;  
:geospatial_lon_min = -154.365997314453 ;  
:geospatial_lat_units = "degrees_north" ;  
:geospatial_lon_units = "degrees_east" ;  
:geospatial_lat_resolution = "289.894507 m" ;  
:geospatial_lon_resolution = "289.894507 m" ;  
:spatialResolution = "289.894507 m" ;  
:data_bins = 7755402LL ;  
:percent_data_bins = 0.1274931f ;  
:units = "CI_stumpf:sr^-1,CI_cyano:sr^-1,CI_noncyano:sr^-1,MCI_stumpf:sr^-1,chl_mph:mg m^-3,flags_mph:undefined,flags_habs:undefined" ;  
:binning_scheme = "Integerized Sinusoidal Grid" ;  
:project = "Ocean Biology Processing Group (NASA/GSFC/OBPG)" ;  
:institution = "NASA Goddard Space Flight Center, Ocean Ecology Laboratory, Ocean Biology Processing Group" ;  
:standard_name_vocabulary = "CF Standard Name Table v36" ;  
:Conventions = "CF-1.6 ACDD-1.3" ;  
:naming_authority = "gov.nasa.gsfc.sci.oceandata" ;  
:id = "L2022206.L3b_DAY_CYANV6T.nc/L3/L2022206.L3b_DAY_CYANV6T.nc" ;  
:license = "https://science.nasa.gov/earth-science/earth-science-data/data-information-policy/" ;  
:creator_name = "NASA/GSFC/OBPG" ;  
:publisher_name = "NASA/GSFC/OBPG" ;  
:creator_email = "data@oceancolor.gsfc.nasa.gov" ;  
:publisher_email = "data@oceancolor.gsfc.nasa.gov" ;  
:creator_url = "https://oceandata.sci.gsfc.nasa.gov" ;  
:publisher_url = "https://oceandata.sci.gsfc.nasa.gov" ;  
:processing_level = "L3 Binned" ;  
:cdm_data_type = "point" ;  
:history = "l3bin par=L2022206.L3b_DAY_CYANV6T.param\n[2025-02-01T03:55:29] ncattredit.py  
L2022206.L3b_DAY_CYANV6T.nc ./L3BATTRIB.txt" ;  
:title = "Level-3 Binned Data" ;  
:instrument = "OLCI" ;  
:platform = "Sentinel-3A,Sentinel-3B" ;  
:source = "satellite observations from OLCI on Sentinel-3A & Sentinel-3B" ;  
  
group: level-3_binned_data {  
    types:
```

```

compound binListType {
    uint64 bin_num ;
    short nobs ;
    short nsenes ;
    float weights ;
    float time_rec ;
}; // binListType
compound binDataType {
    float sum ;
    float sum_squared ;
}; // binDataType
compound binIndexType {
    uint64 start_num ;
    uint64 begin ;
    uint extent ;
    uint64 max ;
}; // binIndexType
dimensions:
    binListDim = UNLIMITED ; // (7755402 currently)
    binDataDim = UNLIMITED ; // (7755402 currently)
    binIndexDim = UNLIMITED ; // (69120 currently)
variables:
    binListType BinList(binListDim) ;
    binDataType CI_stumpf(binDataDim) ;
    binDataType CI_cyano(binDataDim) ;
    binDataType CI_noncyano(binDataDim) ;
    binDataType MCI_stumpf(binDataDim) ;
    binDataType chl_mph(binDataDim) ;
    binDataType flags_mph(binDataDim) ;
    binDataType flags_habs(binDataDim) ;
    binIndexType BinIndex(binIndexDim) ;
} // group level-3_binned_data

group: processing_control {

// group attributes:
    :software_name = "L3BIN" ;
    :software_version = "5.14" ;
    :input_sources =
"S3A_OLCI_EFRNT.20220725.L3b.DAY.CYANV6T.nc,S3B_OLCI_EFRNT.20220725.L3b.DAY.CYANV6T.nc
";
    :l2_flag_names = "LAND,CLDICE,HISATZEN" ;

group: input_parameters {

// group attributes:
    :infile = "/data2/sdpsoper/vdc/vpu1/workbuf/l3inlist.dat" ;
    :ofile = "L2022206.L3b_DAY_CYANV6T.nc" ;
    :pfile = "L2022206.L3b_DAY_CYANV6T.nc" ;
    :offormat = "netCDF4" ;
    :syear = "9999" ;
    :eyear = "9999" ;
    :sday = "1970001" ;
    :eday = "2038018" ;
    :sorbit = "-1" ;
    :eorbit = "-1" ;
}

```

```
:out_parm = ":DEFAULT:" ;
:processing_version = "6T" ;
:reduce_fac = "1" ;
:resolve = "" ;
:merged = "" ;
:loneast = "180.000000" ;
:lonwest = "-180.000000" ;
:latnorth = "90.000000" ;
:latsouth = "-90.000000" ;
:verbose = "0" ;
:unit_wgt = "0" ;
:median = "0" ;
:deflate = "4" ;
:composite_prod = "CI_cyano" ;
:composite_scheme = "max" ;
:doi = "10.5067/MERGED-S3/OLCI/L3B/CYAN/CI/6T" ;
} // group input_parameters
} // group processing_control
}
```

Appendix B: CyAN daily merged OLCI metadata V5

```
netcdf L2022206.L3b_DAY_CYAN {  
  
    // global attributes:  
    :product_name = "L2022206.L3b_DAY_CYAN.nc" ;  
    :temporal_range = "7-hour" ;  
    :start_orbit_number = 22127 ;  
    :end_orbit_number = 33524 ;  
    :date_created = "2022245032405000" ;  
    :processing_version = "CYAN-v4.0" ;  
    :source = "satellite observations from OLCI-Sentinel-3A" ;  
    :time_coverage_start = "2022-07-25T13:35:09.000Z" ;  
    :time_coverage_end = "2022-07-25T20:10:06.000Z" ;  
    :northernmost_latitude = 62.87891f ;  
    :southernmost_latitude = 8.279948f ;  
    :easternmost_longitude = -45.15788f ;  
    :westernmost_longitude = -154.3724f ;  
    :geospatial_lat_max = 62.87890625 ;  
    :geospatial_lat_min = 8.27994823455811 ;  
    :geospatial_lon_max = -45.1578750610352 ;  
    :geospatial_lon_min = -154.372421264648 ;  
    :geospatial_lat_units = "degrees_north" ;  
    :geospatial_lon_units = "degrees_east" ;  
    :geospatial_lat_resolution = "289.894507 m" ;  
    :geospatial_lon_resolution = "289.894507 m" ;  
    :spatialResolution = "289.894507 m" ;  
    :data_bins = 11381441LL ;  
    :percent_data_bins = 0.1871025f ;  
    :units = "CI_stumpf:sr^-1,CI_cyano:sr^-1,CI_noncyano:sr^-1,MCI_stumpf:sr^-1,chl_mph:mg m^-3,flags_mph:undefined,flags_habs:undefined" ;  
    :binning_scheme = "Integerized Sinusoidal Grid" ;  
    :project = "Ocean Biology Processing Group (NASA/GSFC/OBPG)" ;  
    :institution = "NASA Goddard Space Flight Center, Ocean Ecology Laboratory, Ocean Biology Processing Group" ;  
    :standard_name_vocabulary = "CF Standard Name Table v36" ;  
    :Conventions = "CF-1.6 ACDD-1.3" ;  
    :naming_authority = "gov.nasa.gsfc.sci.oceandata" ;  
    :id = "L2022206.L3b_DAY_CYAN.nc/L3/L2022206.L3b_DAY_CYAN.nc" ;  
    :license = "https://science.nasa.gov/earth-science/earth-science-data/data-information-policy/" ;  
    :creator_name = "NASA/GSFC/OBPG" ;  
    :publisher_name = "NASA/GSFC/OBPG" ;  
    :creator_email = "data@oceancolor.gsfc.nasa.gov" ;  
    :publisher_email = "data@oceancolor.gsfc.nasa.gov" ;  
    :creator_url = "https://oceandata.sci.gsfc.nasa.gov" ;  
    :publisher_url = "https://oceandata.sci.gsfc.nasa.gov" ;  
    :processing_level = "L3 Binned" ;  
    :cdm_data_type = "point" ;  
    :history = "l3bin par=L2022206.L3b_DAY_CYAN.param\n[2022-09-02T04:06:16] ncattredit.py  
L2022206.L3b_DAY_CYAN.nc ./L3BATTRIB.txt" ;  
    :title = "Level-3 Binned Data" ;  
    :instrument = "OLCI" ;  
    :platform = "Sentinel-3A,Sentinel-3B" ;  
  
    group: level-3_binned_data {
```

```

types:
compound binListType {
    uint64 bin_num ;
    short nobs ;
    short nscenes ;
    float weights ;
    float time_rec ;
}; // binListType
compound binDataType {
    float sum ;
    float sum_squared ;
}; // binDataType
compound binIndexType {
    uint64 start_num ;
    uint64 begin ;
    uint extent ;
    uint64 max ;
}; // binIndexType
dimensions:
binListDim = UNLIMITED ; // (11381441 currently)
binDataDim = UNLIMITED ; // (11381441 currently)
binIndexDim = UNLIMITED ; // (69120 currently)
variables:
binListType BinList(binListDim) ;
binDataType CI_stumpf(binDataDim) ;
binDataType CI_cyano(binDataDim) ;
binDataType CI_noncyano(binDataDim) ;
binDataType MCI_stumpf(binDataDim) ;
binDataType chl_mph(binDataDim) ;
binDataType flags_mph(binDataDim) ;
binDataType flags_habs(binDataDim) ;
binIndexType BinIndex(binIndexDim) ;
} // group level-3_binned_data

group: processing_control {

// group attributes:
:software_name = "L3BIN" ;
:software_version = "5.13" ;
:input_sources =
"S3A_OLCI_EFRNT.20220725.L3b.DAY.CYANV4.nc,S3B_OLCI_EFRNT.20220725.L3b.DAY.CYANV4.nc" ;
:l2_flag_names = "LAND,CLDICE,HISATZEN" ;

group: input_parameters {

// group attributes:
:infile = "/data8/sdpsoper/vdc/vpu7/workbuf/l3inlist.dat" ;
:ofile = "L2022206.L3b_DAY_CYAN.nc" ;
:pfile = "L2022206.L3b_DAY_CYAN.nc" ;
:oformat = "netCDF4" ;
:syear = "9999" ;
:eyear = "9999" ;
:sday = "1970001" ;
:eday = "2038018" ;
:sorbit = "-1" ;
:eorbit = "-1" ;
}

```

```
:out_parm = ":DEFAULT:" ;
:processing_version = "CYAN-v4.0" ;
:reduce_fac = "1" ;
:merged = "" ;
:loneast = "180.000000" ;
:lonwest = "-180.000000" ;
:latnorth = "90.000000" ;
:latsouth = "-90.000000" ;
:verbose = "0" ;
:unit_wgt = "0" ;
:median = "0" ;
:deflate = "4" ;
:composite_prod = "CI_cyano" ;
:composite_scheme = "max" ;
} // group input_parameters
} // group processing_control
}
```

Appendix C: CyAN MERIS metadata V4

```
netcdf M2010226.L3b_DAY_CYAN {  
  
// global attributes:  
:product_name = "M2010226.L3b_DAY_CYAN.nc" ;  
:title = "MERIS Level-3 Binned Data" ;  
:instrument = "MERIS" ;  
:platform = "Envisat" ;  
:temporal_range = "6-hour" ;  
:start_orbit_number = 44210 ;  
:end_orbit_number = 44213 ;  
:date_created = "2022-06-02T00:52:01.000Z" ;  
:processing_version = "CYAN-v4.0" ;  
:source = "satellite observations from MERIS-Envisat" ;  
:history = "l2bin par=M2010226.L3b_DAY_CYAN.param" ;  
:time_coverage_start = "2010-08-14T14:51:18.000Z" ;  
:time_coverage_end = "2010-08-14T19:58:03.000Z" ;  
:northernmost_latitude = 78.04557f ;  
:southernmost_latitude = 23.89974f ;  
:easternmost_longitude = -46.56836f ;  
:westernmost_longitude = -143.8886f ;  
:geospatial_lat_max = 78.0455703735352 ;  
:geospatial_lat_min = 23.8997402191162 ;  
:geospatial_lon_max = -46.568359375 ;  
:geospatial_lon_min = -143.888610839844 ;  
:geospatial_lat_units = "degrees_north" ;  
:geospatial_lon_units = "degrees_east" ;  
:geospatial_lat_resolution = "289.894507 m" ;  
:geospatial_lon_resolution = "289.894507 m" ;  
:spatialResolution = "289.894507 m" ;  
:data_bins = 6940776LL ;  
:percent_data_bins = 0.1141013f ;  
:units = "CI_stumpf:sr^-1,CI_cyano:sr^-1,CI_noncyano:sr^-1,MCI_stumpf:sr^-1,chl_mph:mg m^-  
3,flags_mph:undefined,flags_habs:undefined,rhos_665:undefined,rhos_560:undefined,rhos_413:undefined" ;  
:binning_scheme = "Integerized Sinusoidal Grid" ;  
:project = "Ocean Biology Processing Group (NASA/GSFC/OBPG)" ;  
:institution = "NASA Goddard Space Flight Center, Ocean Ecology Laboratory, Ocean Biology  
Processing Group" ;  
:standard_name_vocabulary = "CF Standard Name Table v36" ;  
:Conventions = "CF-1.6 ACDD-1.3" ;  
:naming_authority = "gov.nasa.gsfc.sci.oceandata" ;  
:id = "M2010226.L3b_DAY_CYAN.nc/L3/M2010226.L3b_DAY_CYAN.nc" ;  
:license = "https://science.nasa.gov/earth-science/earth-science-data/data-information-policy/" ;  
:creator_name = "NASA/GSFC/OBPG" ;  
:publisher_name = "NASA/GSFC/OBPG" ;  
:creator_email = "data@oceancolor.gsfc.nasa.gov" ;  
:publisher_email = "data@oceancolor.gsfc.nasa.gov" ;  
:creator_url = "https://oceandata.sci.gsfc.nasa.gov" ;  
:publisher_url = "https://oceandata.sci.gsfc.nasa.gov" ;  
:processing_level = "L3 Binned" ;  
:cdm_data_type = "point" ;  
  
group: level-3_binned_data {  
    types:
```

```

compound binListType {
    uint64 bin_num ;
    short nobs ;
    short nscenes ;
    float weights ;
    float time_rec ;
}; // binListType
compound binDataType {
    float sum ;
    float sum_squared ;
}; // binDataType
compound binIndexType {
    uint64 start_num ;
    uint64 begin ;
    uint extent ;
    uint64 max ;
}; // binIndexType
dimensions:
    binListDim = UNLIMITED ; // (6940776 currently)
    binDataDim = UNLIMITED ; // (6940776 currently)
    binIndexDim = UNLIMITED ; // (69120 currently)
variables:
    binListType BinList(binListDim) ;
    binDataType CI_stumpf(binDataDim) ;
    binDataType CI_cyano(binDataDim) ;
    binDataType CI_noncyano(binDataDim) ;
    binDataType MCI_stumpf(binDataDim) ;
    binDataType chl_mph(binDataDim) ;
    binDataType flags_mph(binDataDim) ;
    binDataType flags_habs(binDataDim) ;
    binDataType rhos_665(binDataDim) ;
    binDataType rhos_560(binDataDim) ;
    binDataType rhos_413(binDataDim) ;
    binIndexType BinIndex(binIndexDim) ;
} // group level-3_binned_data

group: processing_control {

    // group attributes:
        :software_name = "l2bin" ;
        :software_version = "7.0.3" ;
        :input_sources = "ENVISAT_MERIS_FRS.20100813T170104.L2.CYAN_CONUS_CYAN-
v4.0.nc,ENVISAT_MERIS_FRS.20100813T170959.L2.CYAN_CONUS_CYAN-
v4.0.nc,ENVISAT_MERIS_FRS.20100813T171309.L2.CYAN_CONUS_CYAN-
v4.0.nc,ENVISAT_MERIS_FRS.20100813T184037.L2.CYAN_CONUS_CYAN-
v4.0.nc,ENVISAT_MERIS_FRS.20100813T184932.L2.CYAN_CONUS_CYAN-
v4.0.nc,ENVISAT_MERIS_FRS.20100814T145118.L2.CYAN_CONUS_CYAN-
v4.0.nc,ENVISAT_MERIS_FRS.20100814T150058.L2.CYAN_CONUS_CYAN-
v4.0.nc,ENVISAT_MERIS_FRS.20100814T163054.L2.CYAN_CONUS_CYAN-
v4.0.nc,ENVISAT_MERIS_FRS.20100814T163949.L2.CYAN_CONUS_CYAN-
v4.0.nc,ENVISAT_MERIS_FRS.20100814T180913.L2.CYAN_CONUS_CYAN-
v4.0.nc,ENVISAT_MERIS_FRS.20100814T181808.L2.CYAN_CONUS_CYAN-
v4.0.nc,ENVISAT_MERIS_FRS.20100814T182125.L2.CYAN_CONUS_CYAN-
v4.0.nc,ENVISAT_MERIS_FRS.20100814T194939.L2.CYAN_CONUS_CYAN-v4.0.nc" ;
        :l2_flag_names = "LAND,CLDICE,HISATZEN" ;
}

```

```

group: input_parameters {
    // group attributes:
        :infile = "/data16/sdpsoper/vdc/vpu15/workbuf/l2inlist.dat" ;
        :ofile = "M2010226.L3b_DAY_CYAN.nc" ;
        :fileuse = "M2010226.L3b_DAY_CYAN.contrib" ;
        :sday = "2010226" ;
        :eday = "2010226" ;
        :latnorth = "90.000000" ;
        :latsouth = "-90.000000" ;
        :loneast = "0.000000" ;
        :lonwest = "0.000000" ;
        :resolve = "Q" ;
        :rowgroup = "270" ;
        :flaguse = "LAND,CLDICE,HISATZEN" ;
        :l3bprod =
    "CI_stumpf,CI_cyano,CI_noncyano,MCI_stumpf,chl_mph,flags_mph,flags_habs,rhos_665,rhos_560,rhos_413" ;
        :output_wavelengths = "ALL" ;
        :prodtype = "O" ;
        :pversion = "CYAN-v4.0" ;
        :suite = "CYAN" ;
        :night = "0" ;
        :verbose = "0" ;
        :minobs = "0" ;
        :delta_crossing_time = "0.000000" ;
        :deflate = "4" ;
        :qual_prod = "" ;
        :composite_prod = "CI_cyano" ;
        :composite_scheme = "max" ;
        :qual_max = "255" ;
    } // group input_parameters
} // group processing_control
}

```